E-ISSN: 2997-9382
American Journal of Technology Advancement
https://semantjournals.org/index.php/AJTA

| Research Article

Check for updates

Synthesis and Characterization of Titanate Nanotubes Via Hydrothermal Process using Temperature Gradient Technique

Mohammed A. Al-Behadili, Abdulwahid A. Al-Hajjaj
Chemical Engineering Department, College of Engineering, University of Basrah
Basrah, Iraq

Annotation

Titanium nanotubes (TiNTs), as a novel nanomaterial, have received abundant attention due to their remarkable structural and functional properties, including a large surface area, excellent biocompatibility, high photochemical capability, and good electronic performance. The hydrothermal method is the most reliable synthetic process for titanate nanotubes, as the entire set of characteristics can be controlled accurately and, more importantly, the synthesis of well-defined nanostructures.

Herein, the synthesis and characterization of titanate nanotubes prepared via hydrothermal reaction using a temperature gradient was described. The experimental process started with the synthesis of TiNTs by hydrothermal reaction at atmospheric pressure. The final samples were further investigated by advanced analytical techniques, such as FTIR, SEM, TEM, and XRD, and all the analyses confirmed the crystalline phase of TiNTs.

The XRD diffraction pattern of the prepared TiNTs was quite different from that of the parent anatase TiNPs. Sharp peaks could be seen at 2θ angles of 27.600°, 36.160°, 41.450°, 54.460°, 62.850°, and 69.200°, corresponding to the crystallographic planes (110), (101), (111), (211), (020), and (301), respectively. The characterizations proved that the well-ordered crystalline structure product was TiNTs, indicating that the proposed hydrothermal synthesis was feasible.

Keywords: titanate nanotubes, hydrothermal synthesis, characterization.

This is an open-access article under the CC-BY 4.0 license

1. Introduction

Titanium-based nanostructures have attracted significant attention in advanced materials research due to their unique physicochemical properties and broad applicability across energy, biomedical engineering, environmental remediation, water treatment, biosensors, and drug delivery systems [1-5]. Titanium nanotubes (TiNTs), a distinct class of one-dimensional nanomaterials derived from titanium dioxide (TiO_2), exhibit a high aspect ratio, excellent ion-exchange capacity, specific interface effects, strong photocatalytic activity, and superior chemical/thermal stability [6-8]. These characteristics are highly dependent on synthesis methods, which have evolved considerably over the past two decades. Several elaborate techniques such as electrochemical anodization, sol-gel process, hydrothermal method, chemical vapor deposition (CVD) and

template directed formation have been used... extensively explored to control TiNT size, morphology, crystallinity, and surface properties [9,10]. Historically, the first electrochemical deposition of TiNTs was reported in 1996 [9,11]. A major breakthrough came in 1998 when Kasuga et al. demonstrated hydrothermal synthesis of TiO_2 and titanate nanotubes from TiO_2 powders under controlled alkaline conditions [12]. This method has since become prominent due to its simplicity, scalability, and ability to produce well-ordered multi-walled nanotubes under mild conditions. In this process, titanium precursors or TiO_2 powders react in concentrated alkaline media (e.g., NaOH or KOH) at elevated temperatures, forming crystalline nanotubular structures through a dissolution-reprecipitation mechanism. Key parameters—including alkali concentration, temperature, reaction duration, and post-synthesis annealing—precisely control nanotube dimensions, crystallinity, and structural integrity [13-17]. For example, Zhou et al. showed that concentrated NaOH solutions yield nanotubes with inner diameters of 5–10 nm [18], while Macak et al. confirmed that annealing at 300–500°C enhances crystallinity and stability [19]. Subsequent studies refined these parameters, examining how reaction time, pH, temperature, and post-treatments affect morphology and surface characteristics [20,21]. Bavykin et al. emphasized hydrothermal treatment as a versatile route for multi-walled titanate nanotubes [22], with Zavala et al. further investigating how HCl washing and annealing temperature influence structure and stability [23]. In recent years, Rempel et al. detailed hydrothermal TiNT synthesis from titanium sources using NaOH/KOH at 100–180°C, followed by acid washing to obtain high-surface-area anatase-phase TiNTs [24]. Fauzi et al. extended this approach to locally sourced ilmenite, producing high-performance nanotubes via NaOH treatment (150°C, 24 hr) and thermal post-processing [25]. Similarly, Alkanad et al. optimized direct hydrothermal synthesis of anatase-phase TiNTs by controlling temperature, time, and precursor ratios, achieving high crystallinity without calcination [26]. As noted by Sengupta and Hussain, hydrothermal/solvothermal methods enable anatase-phase TiNT growth from titanium precursors in alkaline environments [27]. Collectively, these studies demonstrate hydrothermal synthesis as a flexible, eco-friendly, and scalable method for tailoring nanotube morphology. However, limitations persist, including long-term product instability, challenges in producing well-ordered crystalline TiO_2 films, restricted pore size adjustability, and uniformity issues [9]. Further optimization of process parameters—particularly temperature profiles and residence times—could advance this technique. To our knowledge, **no published studies have implemented gradient temperature ramping in hydrothermal TiNT synthesis**. This work therefore investigates the feasibility of synthesizing titanium nanotubes via a gradient-temperature hydrothermal process, with emphasis on structural optimization.

2. Materials and methods

2.1 Materials and chemical reagents

The materials considered Materials The materials used in this work are: TiO2 nanoparticle (TiO2), NaOH, KOH, HCl, and deionized (DI) water. All these materials were analytical grades and obtained from the United States of America and Indian suppliers as listed in Table 1.

Table1. List of materials used and their specifications.

Material	Formula	Molecular mass ($gmol^{-1}$)	Purity
Titanium Dioxide	TiO_2	79.90	99.5%
Sodium Hydroxide	NaOH	40.00	97.5%
Potassium Hydroxide	KOH	56.11	85%
Hydrochloride Acid	HCL	36.46	36.5-38.0%

2.2 Synthesis of titanate nanotubes (TiNTs)

The protonated TiNT (H-TiNT) were fabricated with the help of an ambient-pressure hydrothermal method in the presence of a base. The method consisted of preparing an aqueous alkaline solution containing both sodium hydroxide (NaOH) and potassium hydroxide (KOH). Titanium dioxide (TiO_2) powder was homogeneously dispersed in this alkaline solution in a polytetrafluoroethylene (PTFE) round-bottomed flask [28].

The suspension was stirred for 2 h at 80 °C, then subjected to a 72-h three-step reflux process as follows:

Initial 24-hour period at 100°C

Subsequent 24-hour phase at 120°C

Final 24-hour stage at 140°C

The reaction mixture was cooled to room temperature after the thermal treatment. The material was then washed several times with distilled water until the washing effluent ran neutral into a pH range of 7-8.

The nanotubes were protonated by a slowly addition of a dilute hydrochloric acid solution (HCl) to reach pH 2. The pH was subsequently adjusted to 5 by repeated rinsing with water. The resulting product was filtered and vacuum dried at room temperature for 24 hours.

The whole of the synthesis process of titanate nanotube via temperature-gradient hydrothermal approach was schematically shown in Figure 1.

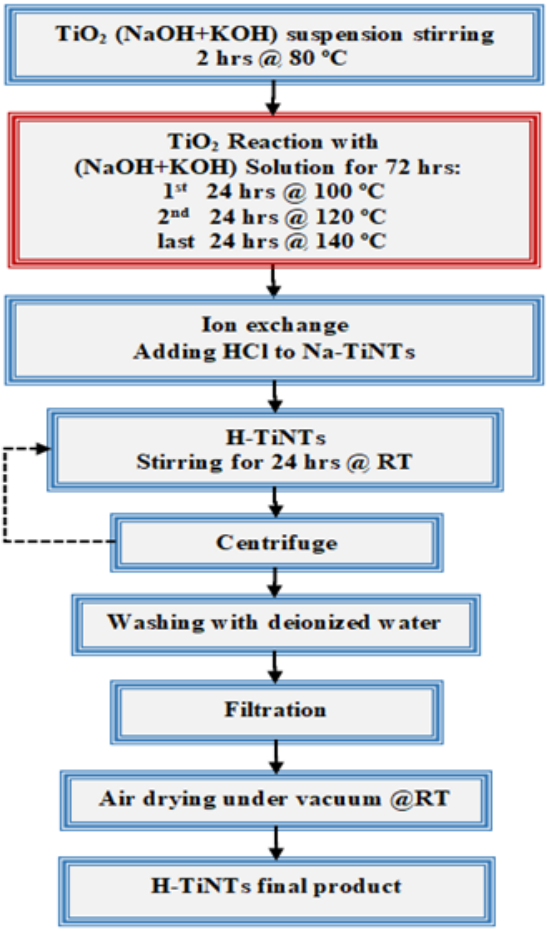

Figure 1. Flow chart of TiNTs synthesis via the temperature gradient hydrothermal process.

2.3. Kinetics characteristics of TiNTs synthesis and formation

The reaction kinetics of TiNT synthesis via hydrothermal treatment is governed by multiple sequential steps, including TiO_2 dissolution, ion exchange, and tubular self-assembly. This kinetics is highly dependent on the reaction parameters, such as temperature, initial concentration, reaction residence time, and pH. Kinetic studies indicate that the formation follows a pseudo-first-order and diffusion-controlled model during the early dissolution phase, whereas the scrolling of titanate layers into tubular structures is driven by minimization of surface free energy. In the dissolution step, the nanostructured TiO_2 dissolution in the aqueous solutions can be achieved by the following possible chemical reactions [29]:

$$TiO_{2(S)} + 4\,H^+ \rightleftharpoons Ti^{4+} + 2H_2O$$

$$TiO_{2(S)} + 2H_2O \rightleftharpoons Ti^{4+} + 4OH^- \quad (2)$$

$$TiO_{2(S)} + 2OH^- \rightleftharpoons TiO_3^{2-} + H_2O$$

The exact form of the Ti^{4+} and TiO_3^{2-} ions may be more complex, including the creation of soluble hydroxides or polytechnic anions. However, one of these processes will dominate dissolution depending on the pH value of the aqueous solution [30].

At high pH values and temperature, TiO_2 reacts with NaOH to form sodium titanate ($Na_2Ti_3O_7$ or Na_2TiO_3) according to the flowing reaction:

$$nTiO_2\,(s) + 2NaOH\,(aq) \rightarrow Na_2Ti_nO_{(2n+1)}\,(s) + H_2O \quad (3)$$

During recrystallization and layer formation steps, the sodium titanate ($Na_2Ti_3O_7$) synthesized through the reaction in Equation (3) starts to form layered nanosheets. These layers are soft and flexible under hydrothermal conditions [23,31]. The scrolling and tubular growth occurs via layer scrolling kinetics, driven by strain minimization and surface tension. in this step, upon aging or mild heating the titanate nanosheets grow anisotropic ally and rearrange into single or multi-walled TiO_2 nanotubes, typically with amorphous walls.

The cation-exchange reaction is required for the conversion from $Na_2Ti_3O_7$ to $H_2Ti_3O_7$. This method of protonation was adapted from prior work [32,33] and was performed in the standard ambient temperature (25°C, 1 atmosphere pressure).

At the time frame of 2 h, it is crucial $Na_2Ti_3O_7$ was exposed to a diluted HCl aqueous solution to exchange sodium Na^+ cations with the hydronium (H_3O^+) ions in the titanate structure. This ionic substitution can be designated by the chemical transformation given by equation (4).

$$Na_2Ti_3O_7\,(s) + 2HCl\,(aq) \rightarrow H_2Ti_3O_7\,(s) + 2NaCl\,(aq) \quad (4)$$

Bavykin et al. [28] reported that increasing temperature from 110°C to 180°C significantly accelerated the transformation. Furthermore, Sugimoto et al. [30] revealed that the growth rate of TiNTs is also influenced by the type of alkali used, where NaOH yields higher dissolution kinetics compared to KOH. Overall, the hydrothermal kinetics obey Arrhenius behavior, and the optimum nanotube formation occurs under balanced thermodynamic and kinetic control to prevent over etching or incomplete scrolling.

The TiNTs used in the present work has been prepared and synthesized via hydrothermal process using temperature gradient technique. Applying a temperature gradient during the hydrothermal process can influence the nucleation and growth rates as the temperatures gradient can lead to variations in the morphology, crystallinity, and surface properties of the nanotubes. It allows for the controlled growth of TiNTs with tailored properties. By adjusting the temperature gradient, it can fine-tune the dimensions (diameter, length) and structure (e.g., nanotube wall thickness) of TiNTs. Achieving the desired morphology and properties requires precise control over the temperature gradient and other synthesis parameters. The temperature gradient can also affect the

crystallinity and phase composition (e.g., anatase, rutile) of TiNTs, which are critical for their photocatalytic and electronic properties

3. Characterization of TiNPs and TiNTs samples

In this section, the formation and structural confirmation of raw TiNPs and TiNTs is addressed. The produced nanotubes have been synthesized in the laboratories of the Chemical Engineering Department, Basrah University using a well-regulated hydrothermal synthesis method with temperature fluctuation to result in similar structural properties and high purity of materials. Material characterization Utilizing advance analytical techniques such as:

FTIR (Fourier-transform infrared spectroscopy)

SEM (scanning electron microscopy)

TEM (transmission electron microscopy)

and X-ray diffraction analysis (XRD), were used to examine their physical and morphological structure.

3.1 Fourier transform infrared (FTIR) spectroscopy

The functional groups and molecular bonds for the fabricated nanomaterials were analyzed by Fourier-transform infrared (FTIR) spectroscopy, confirming the chemical change from TiO_2 to titanium nanotubes. The FTIR spectra are displayed in Figure 2 where the spectrum for titanium NPs is shown in panel a) and the nanotubes in panel b).

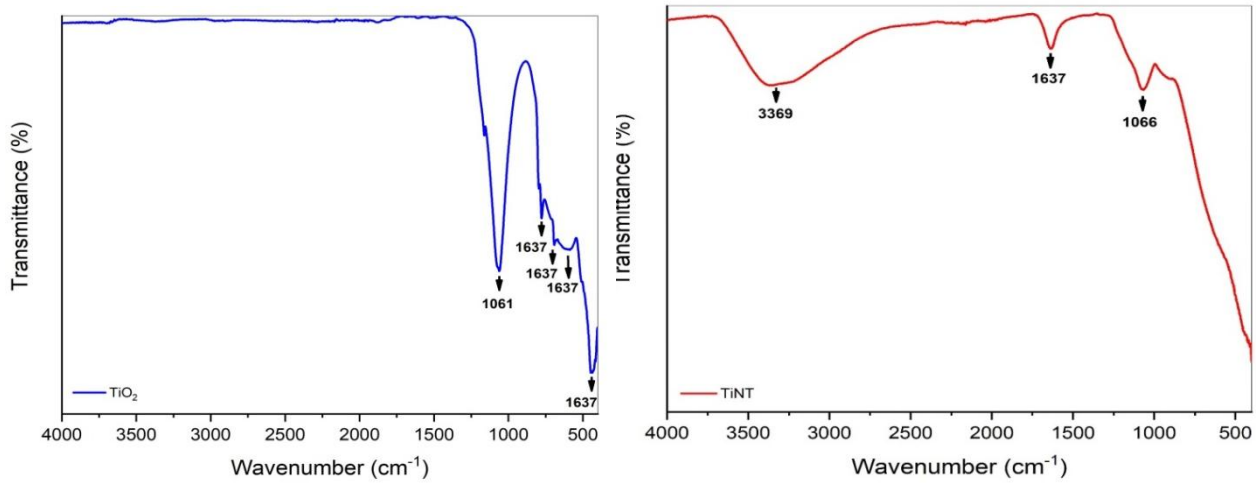

Figure 2. (a) FTIR spectrum of TiNPs, (b) FTIR spectrum of TiNTs.

Figure 2b shows the FTIR spectra of hydrothermal-treated titanium nanotubes (TiNTs) with bands of absorption in the region of wavenumbers from 500 to 4000 cm^{-1}. A number of characteristic vibrational modes were observed:

Strong bands of 3208.0046 cm^{-1}correspond to the stretching of O-H bond vibration(logits) 2.5.2.2.

The peak at 1618.948 cm^{-1} originates from the bending modes of Ti-OH due to the water molecules.

The absorption peak at 1482.0269 cm^{-1} is attributed to the Ti-O-Ti stretching vibrations.

Some other distinguishable sharp peaks are also present at 1066 cm^{-1}, 1637 cm^{-1}, and 3369 cm^{-1}, which are original band of TiNTs, strongly illustrating that the obtained TiNTs are formed successfully and confirm our material was highly pure.

3.2 SEM and TEM characterizations

Scanning Electron Microscopy (SEM)

SEM is an imaging technique using intense electron source from thermionic or field-emission types This method generates detailed topographical maps via electron-sample interactions.

Transmission Electron Microscopy (TEM)

TEM is based upon an entirely different principle by taking a coherent electron beam of uniform current density produced by thermionic, Schottky and field-emission sources [34, 35]. This radiation propagates through the ultra-thin samples, and provides high-resolution images of this internal structure.

Voltage Classification of Electron Microscopes:

Conventional-voltage instruments: Operating range from 80-120 kV acceleration voltages

Intermediate-voltage systems: Work in the range of 120-500 kV, with higher resolution

High Voltage apparatus: Operable between 500 - 3000 kV for superior resolution of further specialized applications

In Figure (3a) SEM image of TiNPs has been shown, which obviously demonstrates their spherical shape with minimal aggregation. Furthermore, it can be seen clearly that all of the particles were nano-sized. Figure (3b) provides a SEM images of TiNTs. The image shows randomly arranged nanotubes which is a characteristic of hydrothermal synthesis. Also, very few spherical particles are observed which illustrate the presence of the unconverted of the TiO_2 nano particle powder. The encircled portion gives the image of a high aspect ratio single nanotube almost 200 nm long.

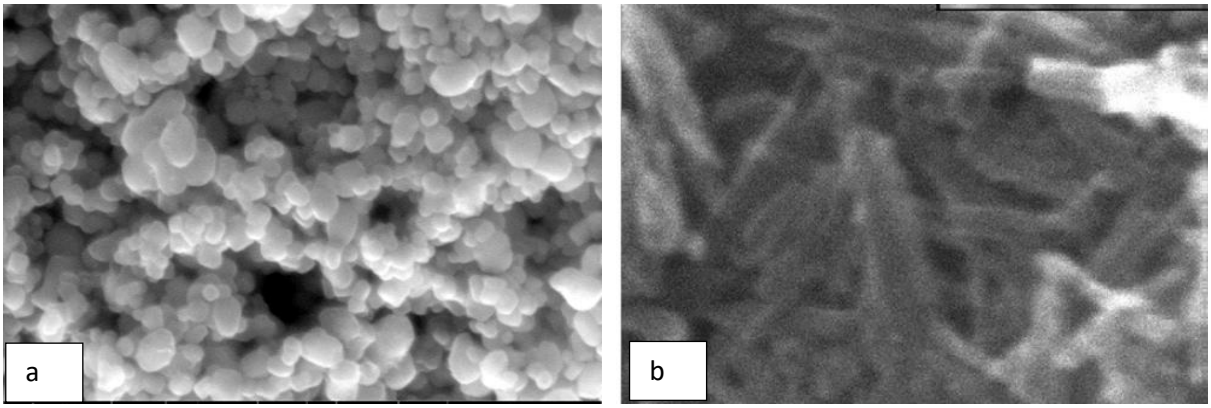

Figure 3. EM images of (a) TiNPs and (b) TiNTs

A titanium-based nanoparticle of nanoscale associated to the anatase crystalline form can be observed by TEM (Figure 4a). These nanoparticles are spherical with an average particle size of about 40 nm, which is evidently observed in the micrograph.

The TEM image (Figure 4b) clearly shows the tubular appearance of the fabricated titanium NTs. The micrograph distinctly shows:

Characteristic hollow cylindrical structures

Considerable length-to-width ratios

Average dimensions about 120-150 nm in length

Diameters varying between 25-30 nm

The nanotubes are haphazardly oriented, indicating that they were formed by a hydrothermal method.

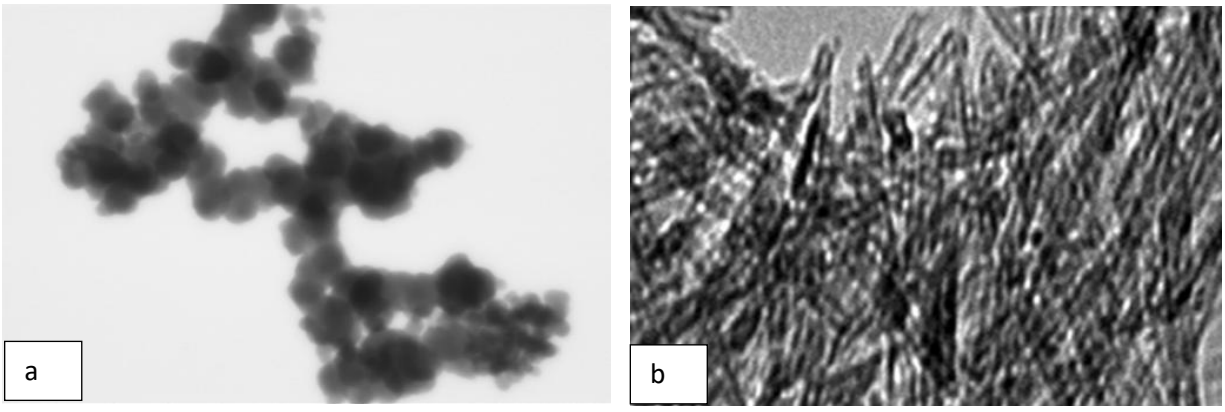

Figure 4. TEM images of (a) TiNPs and (b) TiNTs

3.3 X-Ray Diffraction (XRD)

X-ray diffraction (XRD) serves as a powerful analytical method for examining material structural characteristics, including:

✓ Crystallinity level

✓ Phase composition

✓ Structural purity

✓ Crystalline domain dimensions

This technique yields crucial data regarding the crystalline phases present and the structural quality of titanium dioxide nanostructures. During analysis, diffracted X-ray intensities are measured while systematically varying:

1. The diffraction angle (2θ)
2. Sample positioning

The resulting peak intensities correlate directly with the quantity of crystallographic ally aligned grains. Alternatively, scattering angles can be measured while maintaining a fixed sample position.

For both titanium nanoparticles (TiNPs) and nanotubes (TiNTs), crystallite dimensions can be determined through application of the established Debye-Scherrer equation [36,37]:

$$D_p = \frac{K\lambda}{\beta \cos\theta} \qquad (1)$$

Several important factors are included in the Debye Scherrer equation:

D_p: Mean crystallite size

K: By shape Scherrer constant factor (0.89 0.94)

λ: The incident X-ray wavelength

β: Represents the line broadening at half maximum intensity (FWHM)

θ: Bragg diffraction angle

This series allows the accurate determination of nanocrystalline parameters from X-ray diffraction data.

The XRD patterns of the (a) precursor titanium nanoparticles and their (b) as-synthesized nanotubes are displayed in Figure 5. The diffraction pattern of the NPs presents five typical peaks at:

25.320° (101 crystallographic plane)

37.820° (004 plane)

48.070° (200 plane)

55.040° (211 plane)

62.790° (204 plane)

These diffraction angles closely match previously reported values [38-40] and indicate the anatase crystalline phase of the precursor. According to Table 2, the average size of crystallites was found to be 40.39 for hkl notation and which is the standard Miller indices to identify the crystal plane.

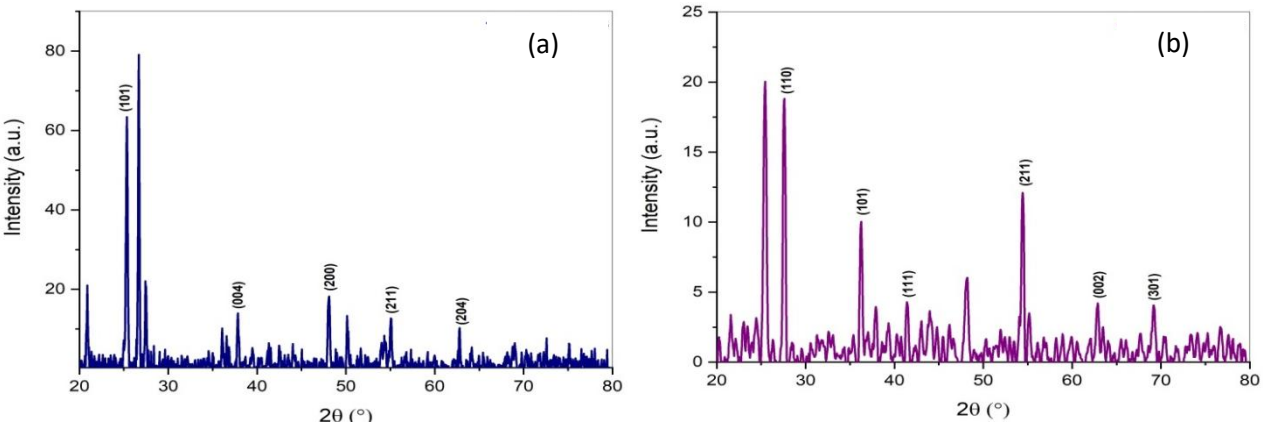

Figure 5. XRD patterns of (a) TiNPs and (b) TiNTs

Table 2. The crystallite size of TiNPs

No.	*2θ (deg.)*	*hkl*	*FWHM (deg.)*	*2θ (rad.)*	*D (nm)*	*Matched by*
1	25.3189	101	0.2263	0.22632	36.007	01-086-1157
2	37.8188	004	0.2263	0.22632	36.007	
3	48.0718	200	0.3168	0.181056	25.480	
4	55.0546	211	0.1811	0.22632	45.008	
5	62.7932	204	0.1358	0.181056	59.452	

As shown in Figure 5b, the X-ray diffraction pattern of the as-synthesized TiNTs exhibits a very different structure from the precursor anatase-phase particles. This change is manifested as a clear change in the crystal phase features. A diffraction pattern with sharp peaks at the following Bragg angles:

27.600° (110 plane)

36.160° (101 plane)

41.450° (111 plane)

54.460° (211 plane)

62.850° (020 plane)

69.200° (301 plane)

These characteristic reflections prove the successful synthesis of crystalline titanate nanotubes having an average crystallite size of 27.30 nm (Table 3). The most intense peak at 27.600°, 54.460°, and 62.85° could be attributed to (110), (211), and (020) crystallography planes, as reported [41].

The diffraction pattern as well show less intense residual peaks of the untransformed TiO_2 nanoparticles, suggesting there are a few quantities of the starting material still present in the final product.

Table 3. The crystallite size of TiNPs

No.	*2θ (deg.)*	*hkl*	*FWHM (deg.)*	*2θ (rad.)*	*D (nm)*	*Matched by*
1	27.6025	110	0.1811	0.22632	30.008	01-078-1510
2	36.1638	101	0.2263	0.22632	29.007	
3	41.4557	111	0.2716	0.22632	25.005	
4	54.4615	211	0.1811	0.22632	30.008	
5	62.8556	020	0.2716	0.22632	25.005	
6	69.208	301	0.2716	0.22632	25.005	

Conclusion

The hydrothermal method has been considered as an excellent and versatile pathway for preparing one-dimensional titanium nanotubes (TiNTs) with well-controlled morphologies and crystalline phases. In particular, application of the temperature gradients during the hydrothermal synthesis has revealed significant effects on both growth dynamics and phase transition of the TiNTs permitting a fine tuning of the dimensional parameters (length and diameter) and the crystalline phase selection (anatase versus titanate).

In this study, the effects of temperature gradient hydrothermal treatment and the ion-exchange of TiNTs on its structure and morphology were systematically examined. The characterization by FTIR (Fourier transform infrared), XRD (X-ray diffraction) and electron microscopy (SEM/TEM) demonstrated that:

The temperature-gradient hydrothermal process is an important factor inducing the growth and structural control of nanotubes.

The crystalline transformation from the initial anatase nanoparticles to the final titanate nanotube structure is caused by the process

The ion exchange serves to ensure a high material purity by replacing sodium ions.

This gradient-temperature hydrothermal strategy provides a versatile synthetic platform to fabricate TiNTs with designed properties, and can be expected to have far-reaching ramifications in both the original research and applications. Further improvement and scale-up of this technique will open up significant technological breakthroughs in various application fields.

References

1. Roy, P., Berger, S., & Schmuki, P. (2011). TiO_2 nanotubes: Synthesis and applications. Angewandte Chemie International Edition, 50(13), 2904–2939.

   https://doi.org/10.1002/anie.201001374

2. Chen, X., & Mao, S. S. (2007). *Titanium dioxide nanomaterials: Synthesis, properties, modifications, and applications.* Chemical Reviews, 107(7), 2891–2959. https://doi.org/10.1021/cr0500535

3. Fujishima, A., Zhang, X., & Tryk, D. A. (2008). *TiO_2 photocatalysis and related surface phenomena.* Surface Science Reports, 63(12), 515–582. https://doi.org/10.1016/j.surfrep.2008.10.001

4. Kaur, M., & Singh, K. (2020). *Recent advances in titanium dioxide-based nanostructures for biomedical and environmental applications.* Nanotechnology Reviews, 9(1), 1306–1324. https://doi.org/10.1515/ntrev-2020-0101
5. Zhou, X., Li, Y., Wang, X., Zhang, L., & Wang, W. (2019). *Recent advances in applications of titanium dioxide nanomaterials: A review.* Environmental Science: Nano, 6(2), 331–365. https://doi.org/10.1039/C8EN00714A
6. Roy, P., Berger, S., & Schmuki, P. (2011). TiO_2 nanotubes: Synthesis and applications. Angewandte Chemie International Edition, 50(13), 2904–2939. https://doi.org/10.1002/anie.201001374
7. Ghosh, S., Basu, S., & Saha, A. (2015). Structure and formation mechanism of titanium oxide nanotubes synthesized by hydrothermal route. Materials Chemistry and Physics, 149, 11–20. https://doi.org/10.1016/j.matchemphys.2014.09.044
8. Zhang, H., & Banfield, J. F. (2000). Understanding polymorphic phase transformation behavior during growth of nanocrystalline aggregates: Insights from TiO_2. The Journal of Physical Chemistry B, 104(15), 3481–3487. https://doi.org/10.1021/jp993819b
9. Liu, N., Chen, X., Zhang, J., & Schwank, J. W. (2013). A review on TiO2-based nanotubes synthesized via hydrothermal method: Formation mechanism, structure modification, and photocatalytic applications. Catalysis Today, 225, 34–51. https://doi.org/10.1016/j.cattod.2013.10.090
10. Mohammed, N. M., Bashiri, R., Sufian, S., Kait, C. F., & Majidai, S. (2018). One-Dimensional titanium dioxide and its application for photovoltaic devices. In InTech eBooks. https://doi.org/10.5772/intechopen.72976
11. Hoyer, P. (1996). Formation of a titanium dioxide nanotube array. Langmuir, 12(6), 1411–1413. https://doi.org/10.1021/la9507803
12. Kasuga, T., Hiramatsu, M., Hoson, A., Sekino, T., & Niihara, K. (1998). Formation of titanium oxide nanotube. *Langmuir*, 14(12), 3160–3163. https://doi.org/10.1021/la9713816
13. Kasuga, T., Hiramatsu, M., Hoson, A., Sekino, T., & Niihara, K. (1998). Formation of titanium oxide nanotube. Langmuir, 14(12), 3160–3163. https://doi.org/10.1021/la9713816
14. Yu, J., & Yu, H. (2006). Facile synthesis and characterization of novel nanocomposites of titanate nanotubes and rutile nanocrystals. Materials Chemistry and Physics, 100(2–3), 507–512. https://doi.org/10.1016/j.matchemphys.2006.02.002
15. Yu, J., Yu, H., Cheng, B., & Trapalis, C. (2006). Effects of calcination temperature on the microstructures and photocatalytic activity of titanate nanotubes. Journal of Molecular Catalysis a Chemical, 249(1–2), 135–142. https://doi.org/10.1016/j.molcata.2006.01.003
16. Bavykin, D. V., Friedrich, J. M., & Walsh, F. C. (2006b). Protonated titanates and TIO2 nanostructured materials: synthesis, properties, and applications. Advanced Materials, 18(21), 2807–2824. https://doi.org/10.1002/adma.200502696
17. Wang, Y., Hu, G., Duan, X., Sun, H., & Xue, Q. (2002). Microstructure and formation mechanism of titanium dioxide nanotubes. Chemical Physics Letters, 365(5–6), 427–431. https://doi.org/10.1016/s0009-2614(02)01502-6
18. Zhou, W., Li, Y., Wang, W., & Song, H. (2001). Formation and characterization of TiO_2 nanotube arrays prepared by hydrothermal process. Chemical Physics Letters, 350(1–2), 6–10. https://doi.org/10.1016/S0009-2614(01)01285-0

19. Macak, J. M., Tsuchiya, H., Ghicov, A., Yasuda, K., Hahn, R., Bauer, S., & Schmuki, P. (2005). TiO_2 nanotubes: self-organized electrochemical formation, properties and applications. Current Opinion in Solid State and Materials Science, 11(1–2), 3–18. https://doi.org/10.1016/j.cossms.2008.01.005

20. Roy, P., Berger, S., & Schmuki, P. (2011). TiO_2 nanotubes: Synthesis and applications. Angewandte Chemie International Edition, 50(13), 2904–2939. https://doi.org/10.1002/anie.201001374

21. Mor, G. K., Varghese, O. K., Paulose, M., Shankar, K., & Grimes, C. A. (2006). A review on highly ordered, vertically oriented TiO_2 nanotube arrays: Fabrication, material properties, and solar energy applications. Solar Energy Materials and Solar Cells, 90(14), 2011–2075. https://doi.org/10.1016/j.solmat.2006.04.007

22. Bavykin, D.V., Kulak, A.N., Walsh, F.C. (2010). Titanate and Titania Nanostructured Materials for Environmental and Electrochemical Applications. Crystal Growth & Design, 10(10), 4421–4427. https://doi.org/10.1021/cg100622h

23. Zavala, M. Á. L., Morales, S. a. L., & Ávila-Santos, M. (2017b). Synthesis of stable TiO2 nanotubes: effect of hydrothermal treatment, acid washing and annealing temperature. Heliyon, 3(11), e00456. https://doi.org/10.1016/j.heliyon.2017.e00456

24. Rempel, A. A., Valeeva, A. A., Vokhmintsev, A. S., & Weinstein, I. A. (2021). Titanium dioxide nanotubes: synthesis, structure, properties and applications. Russian Chemical Reviews, 90(11), 1397–1414. https://doi.org/10.1070/rcr4991

25. Fauzi, A., Lalasari, L. H., Sofyan, N., Ferdiansyah, A., Dhaneswara, D., & Yuwono, A. H. (2022). Synthesis of titanium dioxide nanotube derived from ilmenite mineral through post-hydrothermal treatment and its photocatalytic performance. Eastern-European Journal of Enterprise Technologies, 2(12 (116)), 15–29. https://doi.org/10.15587/1729-4061.2022.255145

26. Alkanad, K., Hezam, A., Al-Zaqri, N., Bajiri, M. A., Alnaggar, G., Drmosh, Q. A., Almukhlifi, H. A., & Krishnappagowda, L. N. (2022). One-Step hydrothermal synthesis of anatase TIO2 nanotubes for efficient photocatalytic CO2 reduction. ACS Omega, 7(43), 38686–38699. https://doi.org/10.1021/acsomega.2c04211

27. Sengupta, J., & Hussain, C. M. (2025). Advancements in Titanium Dioxide Nanotube-Based Sensors for Medical Diagnostics: A Two-Decade Review. Nanomaterials, 15(13), 1044. https://doi.org/10.3390/nano15131044

28. Al-Behadili M.A., Al-Hajjaj A.A. (May, 2025); Applications of Nano-Materials in Heat Exchangers: Recent Advances & Prospects; International Journal of Advances in Engineering Research, Vol 29, Issue 5, 9-26. https://www.ijaer.com/past_paper.php?volid=166

29. Bavykin, D. V., Friedrich, J. M., & Walsh, F. C. (2006). Protonated titanate and TiO2 nanostructured materials: synthesis, properties, and applications. Advanced Materials, 18(21), 2807–2824. https://doi.org/10.1002/adma.200502696

30. Bavykin, D. V., Friedrich, J. M., & Walsh, F. C. (2006c). Protonated titanates and TIO2 nanostructured materials: synthesis, properties, and applications. Advanced Materials, 18(21), 2807–2824. https://doi.org/10.1002/adma.200502696

31. Wei, M., Konishi, Y., Zhou, H., Sugihara, H., & Arakawa, H. (2004). A simple method to synthesize nanowires titanium dioxide from layered titanate particles. Chemical Physics Letters, 400(1–3), 231–234. https://doi.org/10.1016/j.cplett.2004.10.114

32. Ivekovic D., Gajovic A., Ceh M., Pihlar B., Electroanalysis 22 (2010) 2202–2210. https://doi.org/10.1002/elan.201090028

33. Al-Hajjaj, A., Zamora, B., Bavykin, D., Shah, A., Walsh, F., & Reguera, E. (2011). Sorption of hydrogen onto titanate nanotubes decorated with a nanostructured Cd3[Fe (CN)6]2 Prussian Blue analogue. International Journal of Hydrogen Energy, 37(1), 318–326. https://doi.org/10.1016/j.ijhydene.2011.09.094

34. I. A. Ismail, M. Z. Yusoff, F. B. Ismail, and P. Gunnasegaran, "Heat transfer enhancement with nanofluids: A review of recent applications and experiments," International Journal of Heat and Technology, vol. 36, no. 4, pp. 1350–1361, Dec. 2018, doi: 10.18280/ijht.360426.

35. R. Barai, D. Kumar, A. Wankhade, and M. Kilic, "Heat transfer performance of nanofluids in heat exchanger: a review ARTICLE INFO," vol. 9, no. 1, pp. 86–106, 2023, doi: 10.14744/jten.2023.xxxx.

36. Gareso, P. L., Heryanto, H., Sampebatu, E. C., Sampe, N., Palentek, V., Taba, P., Juarlin, E., & Aryanto, D. (2021). Synthesis and material characterization of TiO2 nanoparticles doped with iron (Fe). Journal of Physics Conference Series, 1763(1), 012059. https://doi.org/10.1088/1742-6596/1763/1/012059

37. Alturki, A. M., & Ayad, R. (2019b). Synthesis and Characterization of Titanium Dioxide Nanoparticles with a Dosimetry Study of their Ability to Enhance Radiation Therapy using a Low Energy X-ray Source. Indian Journal of Science and Technology, 12(9), 1–5. https://doi.org/10.17485/ijst/2019/v12i9/140977

38. Kholief, M. G., Hesham, A. E., Hashem, F. S., & Mohamed, F. M. (2024). Synthesis and utilization of titanium dioxide nano particle (TiO2NPs) for photocatalytic degradation of organics. Scientific Reports, 14(1). https://doi.org/10.1038/s41598-024-53617-9

39. Albukhaty, S., Al-Bayati, L., Al-Karagoly, H., & Al-Musawi, S. (2020). Preparation and characterization of titanium dioxide nanoparticles andinvitro investigation of their cytotoxicity and antibacterial activity against Staphylococcus aureus and Escherichia coli. Animal Biotechnology, 33(5), 864–870. https://doi.org/10.1080/10495398.2020.1842751

40. Vats, T., & Sharma, S. N. (2019). Effect of annealing temperature on the structural, morphological and optical properties of TiO_2 nanotubes and their composites with CdSe Quantum dots. Journal of Applied Research and Technology, 17(2). https://doi.org/10.22201/icat.16656423.2019.17.2.806

41. Lu, S., Zhong, H., Mo, D., Hu, Z., Zhou, H., & Yao, Y. (2017). A H-titanate nanotube with superior oxidative desulfurization selectivity. Green Chemistry, 19(5), 1371–1377. https://doi.org/10.1039/c6gc03573f